The nebular spectra of the transitional Type Ia Supernovae 2007on and 2011iv: broad, multiple components indicate aspherical explosion cores

P. A. Mazzali,[1,2]★ C. Ashall,[1,3] E. Pian,[4] M. D. Stritzinger,[5] C. Gall,[5,6]
M. M. Phillips,[7] P. Höflich[3] and E. Hsiao[3]

[1]*Astrophysics Research Institute, Liverpool John Moores University, IC2, Liverpool Science Park, 146 Brownlow Hill, Liverpool L3 5RF, UK*
[2]*Max-Planck-Institut für Astrophysik, Karl-Schwarzschild-Strasse 1, D-85748 Garching, Germany*
[3]*Department of Physics, Florida State Universiy, Tallahassee, FL 32306, USA*
[4]*IASF-Bo, Via PieroGobetti, 101, I-40129 Bologna, Italy*
[5]*Department of Physics and Astronomy, Aarhus University, Ny Munkegade 120, DK-8000 Aarhus C, Denmark*
[6]*Ø Denmark Dark Cosmology Centre, Niels Bohr Institute, University of Copenhagen, Juliane Maries Vej 30, DK-2100 Copenhagen*
[7]*Carnegie Observatories, Las Campanas Observatory, 601 Casilla, La Serena, Chile*

ABSTRACT

The nebular-epoch spectrum of the rapidly declining, 'transitional' Type Ia supernova (SN) 2007on showed double emission peaks, which have been interpreted as indicating that the SN was the result of the direct collision of two white dwarfs. The spectrum can be reproduced using two distinct emission components, one redshifted and one blueshifted. These components are similar in mass but have slightly different degrees of ionization. They recede from one another at a line-of-sight speed larger than the sum of the combined expansion velocities of their emitting cores, thereby acting as two independent nebulae. While this configuration appears to be consistent with the scenario of two white dwarfs colliding, it may also indicate an off-centre delayed detonation explosion of a near-Chandrasekhar-mass white dwarf. In either case, broad emission line widths and a rapidly evolving light curve can be expected for the bolometric luminosity of the SN. This is the case for both SNe 2007on and 2011iv, also a transitional SN Ia that exploded in the same elliptical galaxy, NGC 1404. Although SN 2011iv does not show double-peaked emission line profiles, the width of its emission lines is such that a two-component model yields somewhat better results than a single-component model. Most of the mass ejected is in one component, however, which suggests that SN 2011iv was the result of the off-centre ignition of a Chandrasekhar-mass white dwarf.

Key words: radiative transfer – techniques: spectroscopic – supernovae: general – supernovae: individual: SN 2007on – supernovae: individual: SN 2011iv.

1 INTRODUCTION

Type Ia supernovae (SNe) are thermonuclear explosions of white dwarfs (WD). The majority of these produce luminous transients, and are compatible with the explosion of carbon–oxygen (CO) WDs that approach the Chandrasekhar limit (Mazzali et al. 2007). Details of the accretion and explosion process remain highly controversial, and it is also not clear whether all 'normal' SNe Ia (those which are normally used for cosmology) are the result of a single mechanism.

Various less common subtypes of SNe Ia also exist. It is often debated whether they are part of the same mechanism or the manifestation of different ones. Several scenarios have been developed that are thought to lead to the thermonuclear explosion of a WD

in a single-degenerate (SD) system or of both WDs in a double-degenerate (DD) system. SD scenarios involve a CO–WD accreting H or He from a non-degenerate companion (Whelan & Iben 1973; Livne 1990; Livne & Glasner 1991; Nomoto & Kondo 1991; Woosley & Weaver 1994; Livne & Arnett 1995). DD scenarios envision two WDs with combined mass exceeding the Chandrasekhar limit merging after their orbits shrink via emission of gravitational waves (Iben & Tutukov 1984; Webbink 1984). Although this should lead to the collapse of the resulting massive ONeMg WD (Nomoto 1982), it may result in a thermonuclear explosion if the merger is a 'violent' one (Pakmor et al. 2010). In an extreme case the WDs may suffer a direct collision and explode by compression. This is expected to happen mostly in dense stellar environments such as globular clusters (Rosswog et al. 2009), but it may be aided if their orbits are focused by the presence of a third or fourth system member (Kushnir et al. 2013; Fang, Thompson & Hirata 2017). The details

★ E-mail: p.mazzali@ljmu.ac.uk

of the explosion depend on the masses of the WDs involved, but the morphology of a DD explosion is always expected to be more aspherical than that of a SD explosion. If the collision has non-zero impact parameter, the explosion may lead to a two-component ejecta structure (Dong et al. 2015).

While luminous SN 1991T-like SNe (Filippenko et al. 1992a; Phillips et al. 1992) may just be a 'more efficient' extension of normal SNe Ia (Mazzali, Danziger & Turatto 1995; Sasdelli et al. 2014; Zhang et al. 2016), at the low end of the SN Ia luminosity distribution different mechanisms may be operating. SN 1991bg (Filippenko et al. 1992b; Leibundgut et al. 1993), the prototypical 'fast decliner', and the class that takes its name, which is characterized by spectra showing lines of low-excitation ions (Mazzali et al. 1997), have been suggested to be the product of a merger of two WDs below the Chandrasekhar mass (Pakmor et al. 2011; Mazzali & Hachinger 2012).

SNe that straddle the 1991bg class and the group of normal SNe Ia are known as 'transitional'. They have rapidly evolving light curves, but spectra that are not as peculiar as those of SN 1991bg. Just like the 1991bg class, they tend to occur in non-star-forming galaxies (Ashall et al. 2016a). SN 1986G, which was the first SN Ia observed to show the Ti II absorption complex near 4500 Å which would later become the hallmark of the subluminous 1991bg class (Phillips et al. 1987; Cristiani et al. 1992), can be explained by a low-energy explosion that still has a mass compatible with the Chandrasekhar mass (Ashall et al. 2016a). SN 2003hv (Leloudas et al. 2003), which was singled out for its flat-topped emission line profiles (Motohara et al. 2006) and the noticeable shift of some emission lines (Maeda et al. 2010), was suggested to be a sub-Chandrasekhar-mass explosion based on the behaviour of its light curve and nebular spectra (Mazzali et al. 2011). Finally, based on its apparently double-peaked emission-line profiles, SN 2007on was suggested to be an example of a head-on collision of two WDs (Dong et al. 2015).

Most of these suggestions have been based on the study of nebular emission lines. Nebular spectra are very useful in SN studies as they reveal the properties of the inner ejecta, which are hidden under a blanket of highly opaque material at earlier times.

A late-time spectrum of SN 2007on (Gall et al. 2018) is shown in Fig. 1, where it is compared to a nebular spectrum of the normal, but rapidly declining SN Ia 2004eo (Pastorello et al. 2007). The figure highlights that the two spectra are similar, but SN 2007on, apart from having slightly narrower emission lines, is characterized by double peaks in several emission lines and by a shift in the position of some of the emission peaks. This highlights why SN 2007on stands out in the nebular phase, although it is not particularly peculiar at earlier times (Ashall et al. 2018).

Here the nebular spectrum of SN 2007on is analysed in order to determine the properties of the explosion (Section 2). Section 3 contains a discussion of SN 2007on, and Section 4 an analysis of SN 2011iv, a transitional SN that exploded in the same host galaxy as SN 2007on, conducted with the same criteria. The nebular data used in this paper were presented by Gall et al. (2018).

2 SYNTHETIC MODELS FOR SN 2007ON

The nebular spectrum was modelled using our non-local thermodynamic equilibrium (NLTE) code. The code has been applied to SNe of different types, e.g. SNe Ia (Mazzali et al. 2008) and SNe Ib/c (Mazzali et al. 2010). Details can be found in those and other papers. Briefly, the energy deposited in the SN nebula by the particles emitted by the radioactive decay of ^{56}Ni into ^{56}Co, and hence into ^{56}Fe,
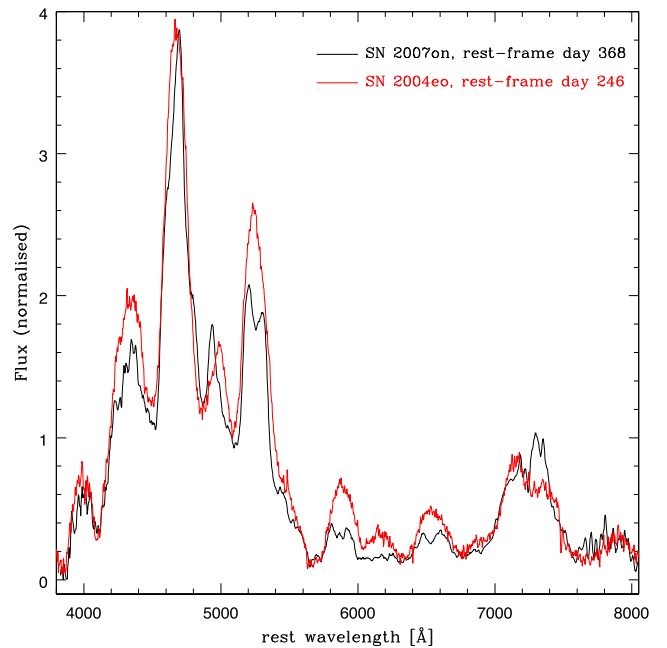

Figure 1. A nebular spectrum of SN 2007on (black) compared to one of SN 2004eo (red). The spectra have been normalized at the peak of the strongest emission line.

is used to heat the SN nebula via collisions. Cooling via (mostly forbidden) line emission balances the heating and gives rise to the observed spectrum. In the case at hand we want to investigate the morphology of the SN ejecta. Therefore, instead of using a stratified density distribution and an explosion model as we did for example in Mazzali et al. (2015), we use a simple one-zone version of the code, which is designed to bring out the most important characteristics of a spectrum and the mass of ^{56}Ni to a good approximation, but cannot be used to estimate the total ejecta mass with great accuracy. This method is however adequate here as a first step to determine the properties of the inner ejecta, which is our main interest in the case of SN 2007on. The discussion below follows the process of investigation, in an attempt to show how we arrived at the solution that is proposed here.

We begin by establishing the basic parameters for the model. The spectrum has been corrected for the recession velocity of the host galaxy (1947 km s^{-1}), with a correction for the specific velocity at the location of the SN (-95 km s^{-1}; Franx, Illingworth & Heckman 1989), resulting in a recession velocity of 1852 km s^{-1}. A distance modulus to the galaxy $\mu = 31.20$ is used, and reddening is assumed to be negligible (Gall et al. 2018). The spectrum was obtained 353 d after B-band maximum. We used a rise time of 17.4 d, as estimated by Gall et al. (2018). This is consistent with rapidly evolving, subluminous SN Ia (Conley et al. 2006; Hayden et al. 2010; Ganeshalingam, Li & Filippenko 2011; Mazzali et al. 2011; Hsiao et al. 2015). We therefore use a rest-frame epoch $t = 368$ d.

Our first attempt was to compute a simple one-zone model to match the entire spectrum. The primary criterion we use to judge our models is their ability to match both the [Fe III]-dominated emission line near 4800 Å and the [Fe II]-dominated emission line near 5200 Å. This is because these are the strongest lines, so that reproducing them should yield the most realistic estimate of the mass of ^{56}Ni. Additionally, because these two lines are dominated by different ionization stages of the same element, reproducing their ratio gives a reasonable estimate of the temperature/density conditions
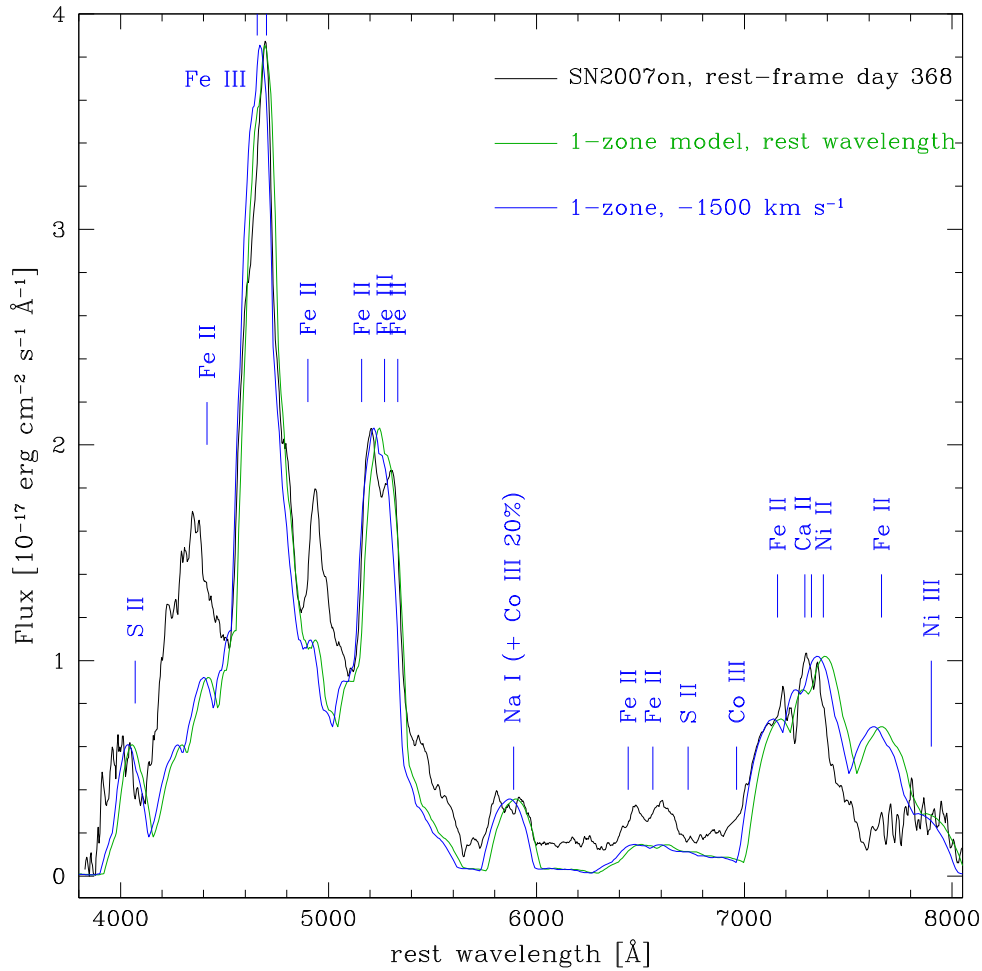
Figure 2. The nebular spectrum of SN 2007on (black) and a one-zone, broad-line model, shown both at rest (green) and with a blueshift of 1500 km s^{-1} (blue).

in the SN nebula. The model we computed is shown in Fig. 2 as a fully drawn (green) line. It has a boundary velocity of 6500 km s^{-1} and it includes 0.19 M$_\odot$ of ^{56}Ni and a total mass of 0.27 M$_\odot$ inside that velocity. We call this the 'broad-line model'. The ^{56}Ni mass is similar to that obtained by Gall et al. (2018) using a simple approximation (0.25 M$_\odot$). The nebular line velocity is small, as expected for a rapidly declining SN Ia (Mazzali et al. 1998, 2007), but it is large for the decline rate of SN 2007on ($\Delta m_{15}(B) = 1.96$ mag, similar to SN 1991bg). We note that Burns et al. (2014) showed that $\Delta m_{15}(B)$ is not a good discriminant at these very fast decline rates. Gall et al. (2018) show that these transitional SNe are better ordered when plotted against the parameter s_{BV}.

As Fig. 2 shows, a one-zone model does not provide a very good fit. The problem is not so much the relative strength of the [Fe II]- and [Fe III]-dominated features – this can be reproduced using a small but not negligible mass of stable Fe ($\approx$0.05 M$_\odot$) and stable Ni ($\approx$0.02 M$_\odot$), which cool the gas, leading to a reduced ionization and suppressed [Fe III] emission – but rather the shape of the various lines, the strongest of which are labelled in the figure. The strongest [Fe III] line near 4700 Å is narrower than the synthetic emission, especially near the peak, but the composite [Fe II]–[Fe III] emission near 5200 Å is broader and bluer than the model line and shows multiple peaks. Line blending and overlap are automatically taken into account by our code. Similar problems are seen in weaker lines: the Na/Co line near 5900 Å (which is dominated by Na I D)

is only reproduced on the red side, while the observed split is clearly not reproduced; the Fe/Ca/Ni structure near 7200 Å is also only approximately reproduced, *although it may be affected by the data reduction process: the sharp absorptions do not seem to be natural for a SN*. Other lines are reproduced in wavelength but not in strength. This affects in particular a number of [Fe II]-dominated features (4400, 4900, 6500, and 6600 Å). A strong [Fe II] emission is predicted near 7600 Å but not observed with a comparable strength. For this and other weak [Fe II] lines the problem may be inaccurate collision strengths. A [S II] line appears to reproduce – at least partially – a line near 4000 Å.

For most SNe Ia, a one-zone model is a good starting approximation, which can then be improved using a stratified model to obtain e.g. a better description of the line profiles. In the case of SN 2007on, however, the discrepancies between the observed spectrum and the one-zone model are too complex to be resolved with a stratified 1D model. This confirms the suggestion of Dong et al. (2015) that multiple components are required. An alternative option may be that the double peaks are caused by self-absorption, but it seems unlikely that SN 2007on is the only SN Ia for which this occurs. Also, not all emissions are affected (and some features are the result of the blend of many lines). SN 1986G showed double peaks on the Na I D line, which was caused by interstellar Na I D absorption in the host galaxy. SN 1986G was heavily reddened, but this is not the case for SN 2007on.
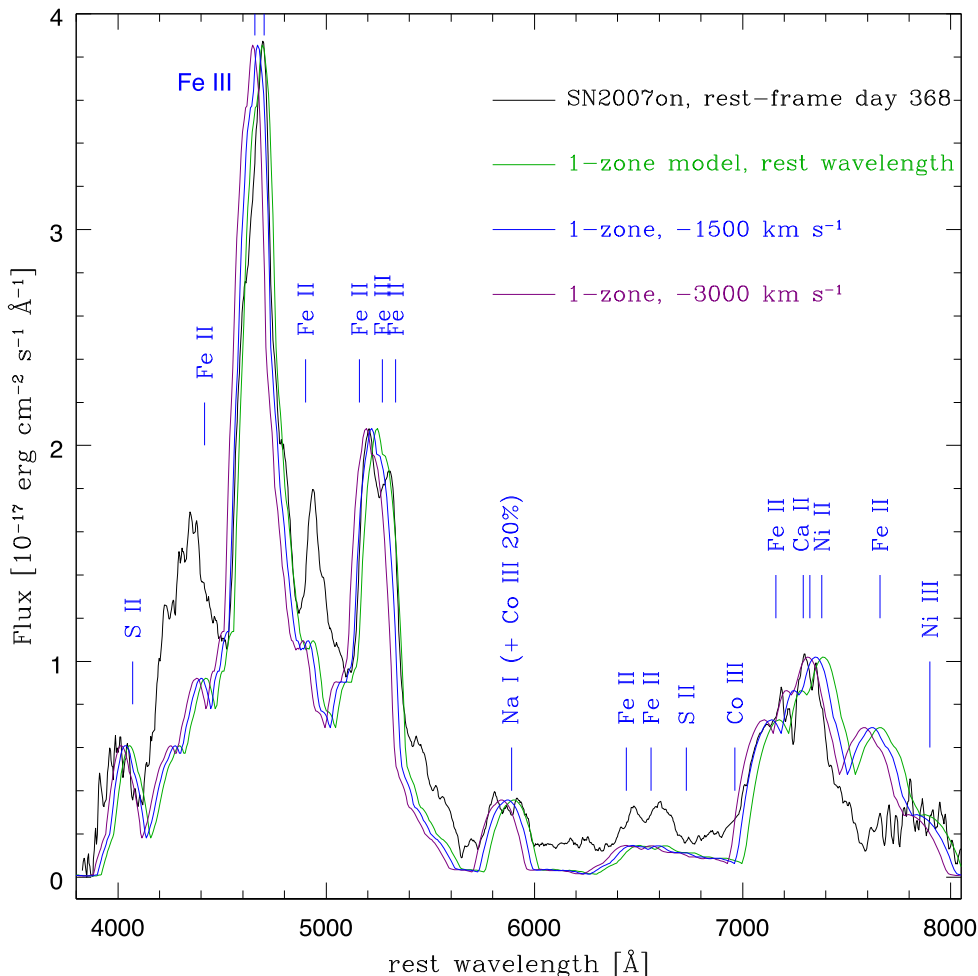
Figure 3. Same as Fig. 2, but now also showing a blueshift of 3000 km s^{-1} (violet line).

In order to figure out how the nebular spectrum of SN 2007on is formed, we began by trying to match the position of the observed lines. First we shifted the one-zone synthetic spectrum bluewards by 1500 km s^{-1}. This is shown in Fig. 2 as a blue line. The blueshifted model now matches the blue side of the 5200 Å emission, including the narrow peak. It also matches the blue side of the emissions at 4700 and 7000–7400 Å, but it is too blue for the 4700 Å peak and not blue enough for the emission at 5900 Å. It matches the [S II] emission near 4000 Å better, while other weaker lines do not change significantly.

In order to match the blue side of the Na I D/[Co III] line a larger blueshift is required. The line coloured in violet in Fig. 3 shows the one-zone synthetic spectrum with a blueshift of 3000 km s^{-1}. With this larger blueshift, emission lines of lighter elements match the data better. This is not just the case for the Na I D/[Co III] line but also for the [S II] line near 4000 Å and the [Ca II] line near 7300 Å, although the contribution of [Ni II] and the possibly spurious narrow absorptions make any conclusions about that feature uncertain. However, all synthetic Fe lines are now too blue.

So, while a multicomponent model seems to be required to explain the spectrum, its details are not immediately inferred just from inspection. It is necessary to decompose the observed spectrum into different components. These may be characterized by narrower emission lines, of width ∼4000 km s^{-1}, matching the width of the narrow emission peaks.

One place to start is to notice that the peaks that are clearly split (e.g. those at 5200 and 5900 Å) show much narrower components. An attempt to fit these is shown in Fig. 4, where we use a single, 'narrow-line' one-zone model. This narrow-line synthetic spectrum is characterized by a width of only 4200 km s^{-1}, matching the width of the narrow emission peaks. This narrow-line synthetic spectrum matches the position of the peaks near 4700 and 7200–7300 Å, but it fails to match either peak of the lines near 5200 and 5900 Å. Additionally, a single narrow-line model is unable to match the high peak ratio of the 4800 versus 5200 Å emissions. This is because the model has rather high density and consequently a low degree of ionization, which favours the Fe II-dominated 5200 Å emission. Only removing elements that cool the gas can cause the ionization to increase, so for example the [S II] emission is poorly reproduced. This means that a simple shift will not work and multiple components with different properties and different shifts in wavelength are needed. We therefore proceed to build a two-component model by combining two separate one-zone models.

We are guided in the construction of a two-component model by the relative shift of the unblended emission peaks. The position of the two emission peaks of the Na I D/[Co III] line indicates an offset of about 6000 km s^{-1}. Fig. 4 shows the narrow-line one-zone model shifted to the red and the blue, respectively, in order to match the emission peaks of the lines near 5200 and 5900 Å. The red dashed line has a redshift of 1500 km s^{-1}. With this redshift the synthetic
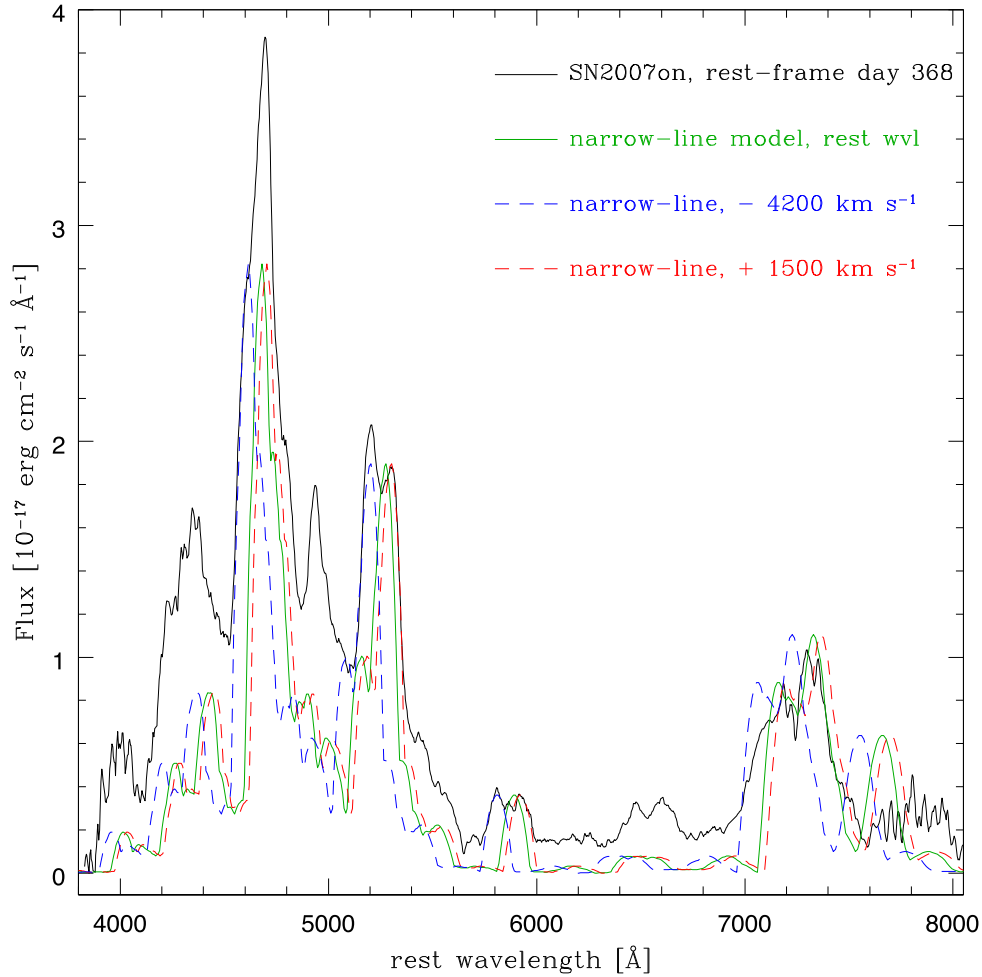
Figure 4. The nebular spectrum of SN 2007on (black) and a narrow-line model shown both at rest (green) and with a blueshift of $4200 \, \mathrm{km \, s^{-1}}$ (dashed, blue line) and a redshift of $1500 \, \mathrm{km \, s^{-1}}$ (dashed, red line) to match narrow features.

spectrum matches in position and width the peaks at 5300 and 5900 Å, which are the red components of the emission features near 5200 and 5850 Å, respectively. The blue dashed line has a blueshift of $4200 \, \mathrm{km \, s^{-1}}$, which matches the bluer peak of the same features. Interestingly, it also matches the blue side of the strong 4700 Å emission and the position of the peak near 4350 Å, confirming that two components with different line-of-sight velocity may be needed to reproduce the observations.

Although shifting the narrow-line one-zone spectrum in wavelength can match the position of different emission peaks, simply summing the blue- and redshifted one-zone spectra to compute a combined spectrum does not match the observations (Fig. 5), although it works amazingly well in places (e.g. the [Fe II]-dominated emission near 5200 Å, the Na I D/[Co III] line near 5900 Å). Yet, this gives us an indication of the kind of procedure we must follow to obtain a fit with a two-component model.

To begin with, the two components cannot be as luminous as what was shown in Figs 4 and 5. Secondly, more emission should be achieved in some of the features that are under-reproduced. This includes [S II] near 4000 Å and several [Fe II]-dominated lines. Conversely, the [Fe II]-dominated emission near 7600 Å should be essentially absent. While increasing the flux of lines of intermediate-mass elements (IMEs) such as S is possible at the cost of a lower temperature, changing the ratios of Fe II transitions is not something

we can manufacture, as it depends on the atomic data that are available. If these are not accurate or complete, we can expect discrepancies between the two-component model and the data.

We built two distinct one-zone models to represent the two different components to the spectrum. The models are characterized by different degrees of ionization. The velocity width of the individual components and their separation were taken as derived above for the narrow-line one-zone model shown in Fig. 4. We computed the two one-zone models iteratively, in an effort to obtain the 'best' solution, but did not attempt to match every detail. Our aim was to explore how well the combination of two components can match the data and to determine the basic physical properties of these components.

Based on the indications above, we need to construct two narrow-line models, each with width $\sim 4000 \, \mathrm{km \, s^{-1}}$, separated by $\sim 5500 \, \mathrm{km \, s^{-1}}$. One model is slightly redshifted ($\sim 1500 \, \mathrm{km \, s^{-1}}$), and the other significantly blueshifted ($\sim 4200 \, \mathrm{km \, s^{-1}}$). From Fig. 5 the blueshifted model is needed to reproduce the blue shoulder in the emission near 4700 Å and the bluer peak in the 5200 Å emission, and it should be very similar to what we used in that figure. The redshifted model, on the other hand, needs to be less luminous, so that the red-side peaks are not overfitted.

The best solution we identified is shown in Fig. 6. The two-component spectra are shown by the blue and red lines, respectively, while the green line is the sum of the two (assuming no radiation
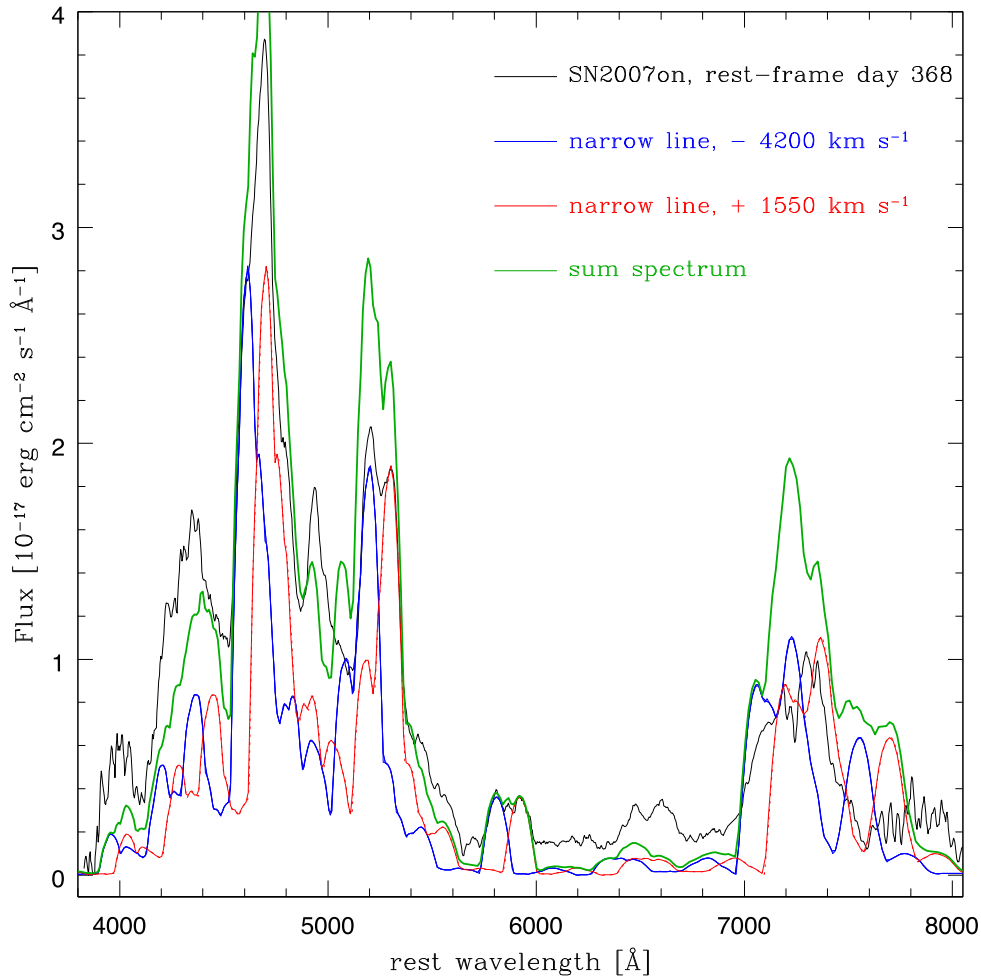
Figure 5. Same as Fig. 4, but now the green line is the sum of the two spectra model.

transport effects). The combination of narrow emission line width and component velocity separation yields a combined emission line width similar to that of the observed spectral features.

One spectrum is blueshifted by $1550\,\mathrm{km\,s^{-1}}$. The nebula that emits this spectrum has $0.084\,\mathrm{M_\odot}$ of $^{56}\mathrm{Ni}$ included within the boundary velocity ($4000\,\mathrm{km\,s^{-1}}$). Additionally, a small amount of stable Ni ($0.003\,\mathrm{M_\odot}$) is required to form the 7380 Å line (which appears near 7250 Å). The presence and strength of this line are uncertain given the probably spurious absorption that affects the data. If some stable Ni is synthesized in the explosion this is typically thought to be at high density near the core of a massive (near-Chandrasekhar mass) CO WD. Some stable Fe is also usually synthesized in this case (see e.g. Iwamoto et al. 1999). Therefore, we also add a small amount of the latter ($0.006\,\mathrm{M_\odot}$). Stable Fe helps to increase the strength of the [Fe II] lines but this is achieved at the cost of a reduced overall ionization balance and therefore a reduced strength of the [Fe III] emission, in particular relative to [Fe II] lines. IMEs must also be present, if the emission line near 4000 Å is blueshifted [S II]. A small amount of S ($0.002\,\mathrm{M_\odot}$) is sufficient for this purpose. As Si and S are usually synthesized together, with a ratio of ~2–3 to 1, we included $0.005\,\mathrm{M_\odot}$ of Si. We also included small amounts (10^{-4}–10^{-3}) of Mg, Ca (useful in the emission complex near 7300 Å), and Na (required for the emission at 5900 Å). This blueshifted spectrum matches only part of the strongest line near 4800 Å, it reproduces the bluer peak of the line at 5200 Å in

position but not in flux, and it successfully matches the blue part of the Na I D/[Co III] emission.

The total mass of this blueshifted nebula, inside the outer boundary velocity ($4000\,\mathrm{km\,s^{-1}}$), is ~$0.10\,\mathrm{M_\odot}$. The outer boundary of the nebula implies that this is just the inner core of the SN ejecta, which is the only part that radiates nebular lines at late times. Fe-group elements are the dominant constituents of this innermost region, as in typical SNe Ia. The mass enclosed within the outer boundary velocity is somewhat small for a SN Ia. The fairly rapidly declining, normal SN Ia 2004eo had ≈$0.23\,\mathrm{M_\odot}$ inside this velocity (Mazzali et al. 2008). On the other hand, subluminous SNe Ia that have been singled out as possibly being the result of different mechanisms have significantly smaller masses: SN 2003hv had ≈$0.05\,\mathrm{M_\odot}$ inside the same velocity (Mazzali et al. 2011), and SN 1991bg had ≈$0.08\,\mathrm{M_\odot}$ (Mazzali & Hachinger 2012).

The second component spectrum in our two-component model is redshifted by $4200\,\mathrm{km\,s^{-1}}$. The nebula that emits this spectrum is quite similar in properties to the one that emits the blueshifted spectrum, but is characterized by a somewhat higher degree of ionization, which is required to match the stronger redshifted component of the [Fe III] emission near 4700 Å. Within an outer boundary velocity of $4200\,\mathrm{km\,s^{-1}}$, which is only marginally larger than the velocity of the blueshifted model, this component includes a similar $^{56}\mathrm{Ni}$ mass as the blueshifted one ($0.084\,\mathrm{M_\odot}$). Unlike the blueshifted model, IMEs in the redshifted model are negligible, but the very small
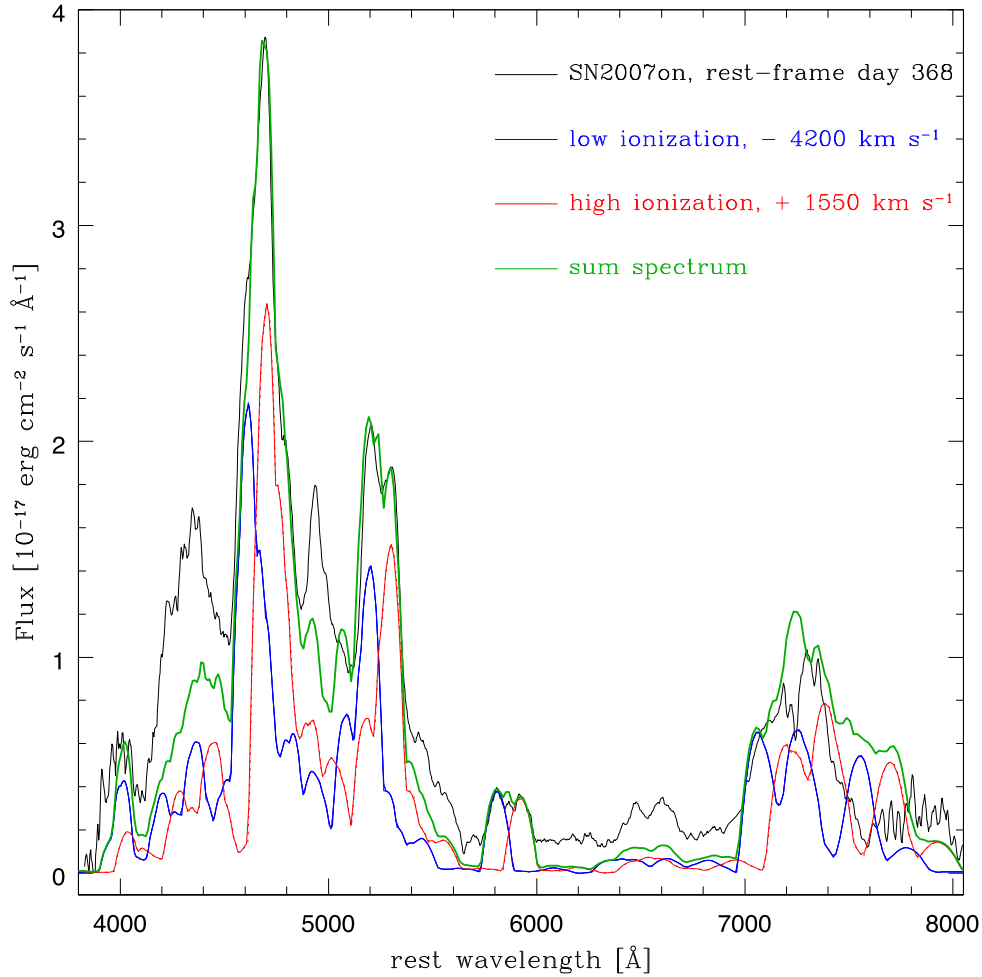
Figure 6. The nebular spectrum of SN 2007on (black) and the two-component model (blue- and redshifted one-zone components are shown in blue and red, respectively) as discussed in the text. The green line is the sum of the two components.

content of Na and Ca (both $\sim 10^{-4}\,M_\odot$) is sufficient to give rise to emission in the intrinsically strongest lines. The low abundance of IMEs is important for obtaining a high degree of ionization, such that the ratio of the two strongest lines favours the [Fe III]-dominated 4700 Å feature more than in the blueshifted model. The ionization state is controlled by the balance of heating and cooling. Heating is provided by ^{56}Ni decay, whereas cooling is provided by line emission. The most important factor influencing ionization is density, and in particular electron density, which controls the recombination rate (which is $\propto \rho^2$). The presence of species that only contribute to cooling but not to heating adds free electrons to the gas and reduces the average ionization because these electrons can recombine with other ions. Hence, in order to keep the ionization high, it helps if the gas is mostly composed of species that contribute to heating and cooling, i.e. radioactive isotopes. Removing stable Fe-group species would also be helpful, but we need to consider the presence of the [Ni II] line. The stable Ni content is $0.004\,M_\odot$, although again establishing its mass from the emission line near 7300 Å is complicated by the shape of the spectrum. The mass of stable Fe is $0.007\,M_\odot$. With a total mass of $\approx 0.10\,M_\odot$ and a slightly larger outer boundary velocity, the densities in the redshifted model are lower than in the blueshifted one, and the ionization degree higher. This leads – as desired – to an Fe III-dominated spectrum, as shown by the ratio of the two strongest lines (red line in Fig. 6). This spectrum matches

only part of the strongest line near 4700 Å and the redder peak of the line at 5200 Å, and it successfully matches the red component of the Na I D/[Co III] emission near 5900 Å. It also reproduces the approximate position of the peaks of the Fe II/Ni II/Ca II complex at 7100–7400 Å.

Similar considerations about the mass of the redshifted component hold as for the blueshifted one (see above). It is small for a normal SN Ia, but it is larger than in both merger and sub-Chandrasekhar models. Neither model seems to reproduce any previously modelled SN Ia (e.g. Mazzali et al. 2008).

A combined spectrum was obtained by summing the two components, neglecting any radiation transport between them. This is both because we assume the gas to be optically thin and, primarily, because we do not know the relative position of the two components with respect to our line of sight. The combined spectrum is shown as a green line in Fig. 6. Most of the complex emission profiles are well reproduced by this spectrum, in shape and wavelength if not always in strength. We could highlight the tiny peak in the centre of the emission line near 5890 Å, which is the result of the sum of two very similar individual parabolic components, but at this low flux level for the observed spectrum we cannot exclude that the agreement with what we see in the data is just a coincidence. Interestingly, also some of the weaker emissions (e.g. the [Fe II]-dominated emissions near 4400 and 6500 Å and the Fe II/Ni II/Ca II

structure at 7200–7500 Å) are much better reproduced by the combined model than by the individual components. This lends further credence to a model for SN 2007on where two separate components contribute to the nebular spectrum. The intensity of several [Fe II] lines is still too weak, and this may have to do with inaccurate atomic data, in particular collision strengths.

Although each component has rather small mass, the combined mass of the two components inside their respective outer boundaries exceeds $0.2\,M_\odot$. This is only slightly smaller than but comparable to a Chandrasekhar-mass explosion with normal energy ($\approx 0.25\,M_\odot$).

3 DISCUSSION: WHAT WAS SN 2007ON?

The nebular spectrum of SN 2007on can be explained assuming it is the sum of two individual components, with similar line width and slightly different density, composition, and ionization degree, receding from one another with a projected line-of-sight velocity of $5750\,\mathrm{km\,s^{-1}}$.

Could these two components be part of the same explosion? It is natural to imagine that they originated at the same time, and this was our modelling assumption. The two one-zone nebulae that we have defined cannot be physically colocated, as they differ in density, composition, and ionization structure. The fact that the boundary expansion velocities of the two nebulae are similar, 4000 and $4200\,\mathrm{km\,s^{-1}}$, respectively, but at the same time the line-of-sight velocity separation is $5750\,\mathrm{km\,s^{-1}}$, suggests that it is possible that the two nebulae are contiguous. The real velocity separation is likely to be larger than $5750\,\mathrm{km\,s^{-1}}$, and could be similar to or larger than the sum of the expansion velocities of the two emitting regions we have modelled, $8200\,\mathrm{km\,s^{-1}}$. In this case these two nebulae, which make the major contribution to the nebular emission, would be separated as bulk, each nebula expanding essentially into free space, independent of the other one. Interestingly, even if the two nebulae were actually moving along the line of sight and their velocity of separation was indeed $5750\,\mathrm{km\,s^{-1}}$, their respective innermost parts, the regions with combined expansion velocities lower than the separation velocity (i.e. $v \sim 2800\,\mathrm{km\,s^{-1}}$), would never come into contact. On the other hand, regions with combined velocities exceeding the separation velocity would interact at some point in the life of the SN. The question then is: Where did the two nebulae come from?

The region that contributes to emission in the nebular phase is only the innermost part of the ejecta of SN 2007on: there is material at higher velocities, containing IMEs in a significant fraction, which gives rise to the early-time spectra of the SN (Ashall et al. 2018; Gall et al. 2018). The mass ejected in SN 2007on is obviously larger than what is included in the individual nebular models. Further information about the outer layers can be obtained from the early phases of the evolution of the SN. In a parallel paper, Ashall et al. (2018) find that the early-time spectra of SN 2007on may be explained by a normal-to-low energy explosion of a Chandrasekhar-mass progenitor.

A scenario that was proposed for SN 2007on is an explosion triggered by the direct collision of two WDs, as outlined by Rosswog et al. (2009) and Kushnir et al. (2013). Kushnir et al. (2013) and following papers do not expect the two WDs to explode independently. On the other hand, they do predict a two-component ejecta structure, which could give rise to some double-peaked emission lines, if the collision occurs with a non-negligible impact parameter (Dong et al. 2015). Raskin et al. (2010) conducted calculations of WD explosions triggered by collisions for different mass ratios, and

found that a large range of ^{56}Ni masses can be obtained for different ratios for the two components, depending on details of the system. The two one-zone components that we used to reproduce the nebular spectrum of SN 2007on have similar ^{56}Ni mass and only slightly different total mass, possibly suggesting also similar masses for the two WDs that may have collided.

As we discussed above, the two emitting regions that the one-zone models define are located in the inner part of the SN ejecta, and their mass – even when combined – should be smaller than the total mass ejected in SN 2007on. Taken individually, the two components have a small mass when compared to the mass enclosed within the same outer boundary velocity of typical Chandrasekhar-mass models. This may suggest that, if the two components correspond to two different WDs, each WD may have had a mass smaller than the Chandrasekhar mass. On the other hand, their combined mass may have been close to it. A 'rebound' of the two components may take place if the collision is not perfectly head-on and the impact parameter is significant (Livne, private communication). If the explosions are independent, the low masses of the two individual components may imply low central densities of the two WDs, which would be in line with the low abundance of neutron-rich nuclear statistical equilibrium (NSE) species deduced for SN 2007on. Any Ni directly observed in a SN Ia spectrum at such advanced epochs must have been synthesized as stable Ni as most radioactive ^{56}Ni will have decayed by then. Stable Fe was used in the models only to match its expected abundance relative to that of stable Ni, but its mass is so small that it does not really affect the thermal balance of the ejecta. Another argument that may be in favour of the collisional scenario is the kinetic energy of the explosion. Ashall et al. (2018) find that SN 2007on may be compatible with a normal explosion energy ($E_K \sim 1$–$1.3 \times 10^{51}\,\mathrm{erg\,s^{-1}}$). Given the rather low kinetic energy yield from thermonuclear burning in a SN that produced little NSE material, having to unbind two low-mass WDs, which would have very low binding energy, would make it easier to balance the energy produced and that observed.

Another possibility may be that in SN 2007on we are witnessing an off-centre ignition of a Chandrasekhar-mass C–O WD that then explodes via a delayed detonation. The total ^{56}Ni mass and other properties of SN 2007on are in line with some of the least energetic delayed detonation models (Höflich et al. 2002; Gall et al. 2018). The lack of stable, neutron-rich NSE species may possibly be explained by a low central density. In the Chandrasekhar-mass scenario, this would require a rapidly rotating WD with low binding energy. The resulting nucleosynthesis, even if it not as effective in producing energy, may be sufficient to unbind the WD and impart it a low E_K, such as what is seen in SN 2007on (Ashall et al. 2018). Achieving a normal or high E_K would however be difficult. The main problem for this scenario is the presence of two distinct sets of lines, and therefore emitting regions, in the nebular spectra. Delayed-detonation models, even in three dimensions, do not seem to produce separate components (e.g. Gamezo, Khokhlov & Oran 2005), nor do models of the violent merger of two sub-Chandrasekhar-mass WDs (e.g. Dan et al. 2015). Some delayed-detonation models characterized by off-centre ignition produce significantly elongated distributions of the Fe-group material, with some expanding at rather high velocity relative to the centre of the WD (Fesen et al. 2007). If observed under a favourable angle, those structures might mimic the behaviour of two individual components. On the other hand, the two nebulae that we need to reproduce the spectrum of SN 2007on seem to have remarkably similar mass. It may not be easy to 'break' the progenitor into two parts of similar mass even in a very off-centre explosion. Additionally, the

very low abundances of stable Fe in SN 2007on may be difficult to achieve in any Chandrasekhar-mass model. In our opinion these are strong arguments against a single, Chandrasekhar-mass progenitor for SN 2007on.

If SN 2007on was indeed the result of the collision of two WDs, or a very off-centre delayed detonation, are there any features other than double-peaked nebular emission line profiles that would make it stand out from the average SN Ia? This is equivalent to asking the question: Could or should we have detected the presence of two separate cores in the early data of SN 2007on? The outer layers of a SN Ia expand at velocities much larger than both the boundary velocities of the nebular emission lines and the separation velocity of the two cores. It is therefore quite likely that at early times the outer layers would just have appeared as one SN explosion (Ashall et al. 2018). Still, if the ^{56}Ni that powers the light curve is indeed located in two distinct components, as indicated by the nebular models, the light curve might be more like the sum of two low-mass ejecta light curves. The two separate ^{56}Ni cores would contribute to the luminosity, but the mean free path from each component would be longer than in the case of a single, central radioactive core. To first order, the light curve may be assumed to be the sum of those of two individual low-mass components, and the diffusion times consequently shorter. The light curve would rise and decline rapidly, but it would be more luminous than the light curve of a SN with similar ^{56}Ni mass concentrated in one place. Thus, one possible signature is a high peak luminosity for the light-curve shape. This is indeed the case for SN 2007on.

Other peculiar aspects of SN 2007on that may be linked to an unusual progenitor/explosion mechanism are as follows.

Its location was outside an elliptical galaxy. Relatively few SNe Ia are observed in elliptical galaxies, and they show a predominance of fast decliners (Hamuy et al. 2000; Howell 2001; Sullivan et al. 2010) and of peculiar events in general (Ashall et al. 2016a). The remote location of SN 2007on may indicate that the progenitor was quite an old system.

The possible detection of X-rays before the explosion (Voss & Nelemans 2008). This was later retracted on positional grounds (Roelofs et al. 2008), but if the detection was real it may have signalled pre-collision/explosion interaction between two WDs. An off-centre delayed detonation would not be expected to show such precursors. Since the detection is quite uncertain, however, it cannot be used as evidence for or against either scenario.

A slowly declining ultraviolet (UV) light curve after maximum (Milne et al. 2010). This may actually be a signature of interaction not so much with a circumstellar medium (CSM), as hypothesized in that paper, but rather of the two colliding ejecta components. This does not mean that the 'beginning' of the interaction was when the light curve started to show a plateau. Interaction should have started at the time of explosion, but its signature may only have become strong when both the densities and the velocities of the interacting material were large enough. The details would differ for the case of collision and off-centre ignition, but at the earliest times the size of the interaction region would be quite small. Additionally, the SN is naturally bright early on, and the added luminosity coming from interaction may only have been appreciable when the SN had become intrinsically dimmer. This is particularly true in the case of an off-centre explosion, in which case the interaction would take place deep within the optically thick ejecta at early times. Only one other SN in the sample of Milne et al. (2010) showed a similar behaviour (actually much more pronounced). This was SN 2005ke, also a subluminous SN Ia.

There may also be other features to look out for, in cases when the double-peak signature is not sufficiently clear (a possible reason for this may be unfavourable orientation). Some possibilities are as follows.

Broad nebular emission lines for the light-curve shape. Most SNe Ia have nebular spectra that are characterized by the same emission lines, with similar ratios, but differing in width. More luminous SNe tend to have broader emission lines, suggesting more complete burning, but the similarity in line ratios indicates that the density is similar in most SNe. Broad emission lines in SNe that are not particularly luminous may indicate the presence of two components separated by too small a line-of-sight velocity to be seen as separate emission peaks or simply not well resolved by the observations. The one-zone fit for the entire spectrum of SN 2007on requires a nebular velocity of 6500 km s^{-1}, which is typical of brighter SNe than SN 2007on. This signature would however also not be detected if the two cores were expanding in a direction perpendicular to our line of sight.

Peculiar light curves. The presence of two nebulae containing ^{56}Ni could be compared to the presence of two SNe. The observed light curve would be some combination of the two components. This would cause a more luminous light curve than the light-curve shape would predict. Interaction between the two ejecta would be additional to this and may affect the UV emission, such as what was seen in SN 2007on, and possibly the X-ray emission as well. In the case of SN 2007on the UV light curve was peculiar in that while in the first 10 d after maximum it declined more rapidly than normal SNe Ia, as did the optical light curves, after this time the decline became slower than what is typical for normal SNe Ia (Milne et al. 2010, fig. 12). Optical bands do not show peculiarities in the case of SN 2007on, but in other cases they might.

Do other SNe Ia share the characteristics and potentially the mechanism of SN 2007on? A search for double-peaked emission has only led to the identification of a handful of potential candidates, SN 2007on being the strongest case (Dong et al. 2015). Of course, detection of double peaks depends on a favourable orientation. There may be SNe that explode through the same mechanism but do not show clearly separated nebular spectra. A possible case is discussed below.

If the collision resulted in two components moving at a large angle with respect to the line of sight, we would not see double peaked emission lines. One possible signature would be the large strength of the emission in rather narrow lines. This case, which represents the majority of the possible orientation angles, may be difficult to appreciate. In any case, for every one SN that shows double peaks there should be several that do not because of unfavourable orientation, suggesting that WD collisions are a non-negligible fraction of at least transitional SNe Ia.

4 WAS SN 2011IV LIKE SN 2007ON?

We have shown that a two-component model appears to be a viable solution for the nebular spectrum of SN 2007on. Another peculiar, transitional SN Ia, SN 2011iv, was discovered in the same passive galaxy in the Fornax cluster and was intensively studied both from the ground (Gall et al. 2018) and with the *Hubble Space Telescope* (Foley et al. 2012). Its location is less remote than SN 2007on: it lies close to the effective radius of the galaxy (Gall et al. 2018). Despite being a rather rapidly declining SN Ia, with $\Delta m_{15}(B) = 1.79$ mag (Gall et al. 2018), which places it at the luminous end of the 1991bg class, SN 2011iv did not show a peculiar spectrum and had a luminosity comparable to that of some underluminous but still
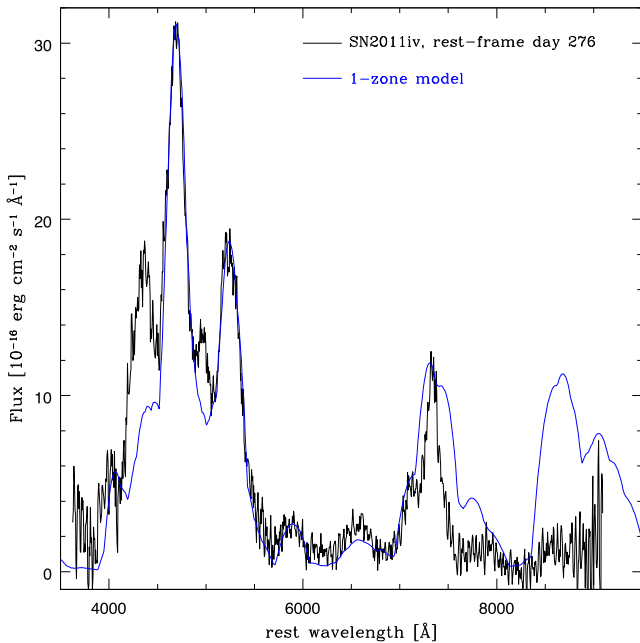
Figure 7. The nebular spectrum of SN 2011iv (black) and a one-zone, broad-line model (blue).

spectroscopically normal SNe Ia such as 2004eo, which have more slowly evolving light curves ($\Delta m_{15}(B) \sim 1.4$–$1.5$ mag; Pastorello et al. 2007; Mazzali et al. 2008).

In a parallel paper, Ashall et al. (2018) perform abundance tomography of SN 2011iv and find that satisfactory agreement can be reached if the SN was a Chandrasekhar-mass, low-energy ($E_K \approx 9 \times 10^{50}$ erg) event that produced $\approx 0.31\,M_\odot$ of ^{56}Ni and a relatively large amount of stable NSE species, especially iron, similar in many ways to SN 1986G (Ashall et al. 2016b). The nebular fit in that paper is good but not perfect. The nebular spectrum of SN 2011iv does not show split or double-peaked emission line profiles, possibly because of a relatively low signal-to-noise ratio, but it does show rather broad emission lines. The spectrum has a lower [Fe III]/[Fe II] peak ratio than that of SN 2007on, indicating a lower overall degree of ionization, similar to SN 2004eo. SN 2011iv satisfies at least two of the criteria laid out above for a double-core event: a high peak luminosity and broad emission lines for its decline rate. Thus motivated, we modelled its nebular spectrum in order to test whether a two-component model can yield an improved fit. We followed the same strategy adopted for SN 2007on above.

We modelled the spectrum obtained 260 d after B maximum (Gall et al. 2018). We used a distance modulus $\mu = 31.20$ as for SN 2007on, and no reddening. Correcting for the rotation of the host galaxy (Scott et al. 2014), the recession velocity at the position of SN 2011iv is 1872 km s^{-1}. Assuming a rise time of 17.9 d, as determined by Gall et al. (2018), we used a rest-frame epoch of 276 d for the spectrum after correcting for time dilation.

We began with a one-zone model, which is shown in Fig. 7. An outer boundary velocity $v = 9000$ km s^{-1} is required to match the observed line width with blends of Fe emission lines. This is a rather high velocity considering the decline rate of the SN. For example, SN 2004eo, whose light-curve decline rate was slower ($\Delta m_{15}(B) = 1.47$ mag; Pastorello et al. 2007), had a line width of $v = 7400$ km s^{-1}. The fit to SN 2011iv required 0.41 $M_\odot$ of ^{56}Ni. Gall et al. (2018) estimate $M(^{56}$Ni$) \approx 0.42\,M_\odot$ from the peak luminosity. The total mass included within the outer boundary is

$\sim 0.80\,M_\odot$. Stable Fe (0.25 $M_\odot$) is the second dominant contribution after ^{56}Ni, followed by stable Ni (0.08 $M_\odot$). Stable Fe-group elements are required to keep the ionization level and the ratio of the two strongest iron emission features low. IMEs also contribute, but their masses are quite small (0.05 $M_\odot$ for Si and S combined).

The biggest problem with building a two-component model is that, unlike the case of SN 2007on, the spectrum does not immediately suggest what the shift of the two components may be or their overall properties. One line that is strikingly shifted with respect to its rest position is the peak near 7300 Å. If that line is Ni II 7380 Å, as is often assumed despite uncertainty caused by blending with other lines such as [Ca II], then the line, which is observed at ≈ 7315 Å after correcting for redshift, is blueshifted by ~ 2700 km s^{-1}. This velocity could be used for one component. The strength of the Ni II emission in that component means that neutron-rich species should have been synthesized there. The presence of these species then implies that this component of the spectrum will likely have rather low ionization. The other component would then need to be more highly ionized in order to reproduce the strong [Fe III] emission peak near 4700 Å. This is a similar situation as in SN 2007on. The 'high-ionization' component needs to be slightly redshifted in order to match the position of the observed emissions. We can optimize the redshift by trying to match the width of the emission peak. Our solution is shown in Fig. 8.

We found that a good solution for the 'low-ionization' component is given by a nebula with boundary velocity $v = 5750$ km s^{-1}, a total mass inside this velocity of 0.46 $M_\odot$, of which M(^{56}Ni)$= 0.26\,M_\odot$, and a blueshift of 2700 km s^{-1}. As in the one-zone model, stable Fe is the second most abundant element (0.12 $M_\odot$), but the mass of stable Ni is relatively small, 0.03 $M_\odot$. With the blueshift that we adopted, the [Ni II] $\lambda7380$ line is now at the wavelength of the observed emission, while other lines match the blue part of the observed features, including the Na I D/[Co II] line. IMEs have small abundances. Their total mass is $\sim 0.05\,M_\odot$. Among these, silicon dominates with 0.03 $M_\odot$.

The mass of this 'low-ionization' nebula within the outer boundary velocity is quite similar to that of a normal Chandrasekhar-mass explosion. Taken on its own, this nebula matches the basic relations that have been found for SNe Ia. The ^{56}Ni content matches the relation between ^{56}Ni mass and light-curve decline rate (Phillips 1993; Phillips et al. 1999; Mazzali et al. 2007) given the decline rate of SN 2011iv. It also would match the relation between decline rate and Fe emission line width (Mazzali et al. 2007) given the ^{56}Ni mass and the decline rate of the SN. However, SN 2011iv was significantly more luminous at peak than those relations would predict: it was about as luminous as SN 2004eo, but had a more rapidly evolving light curve. It also shows broader lines than expected. This is actually quite suggestive. The high peak luminosity and broad emission lines could be due to the presence of a second component, which may affect the post-maximum decline rate because it evolves rapidly. The observed light curve would then be the combination of the two components and could be more luminous that the decline rate would imply. This requires the two components to be well separated, which may be possible, as in the case of SN 2007on.

In order to complete the fit, a second component is needed. This should be of higher ionization, as discussed above, and should contain little to no stable nickel, since the [Ni II] emission is reproduced by the 'low-ionization' nebula alone. This possible 'high-ionization' component does not need to have a very strong flux, and therefore it turns out to be quite small in mass. In our
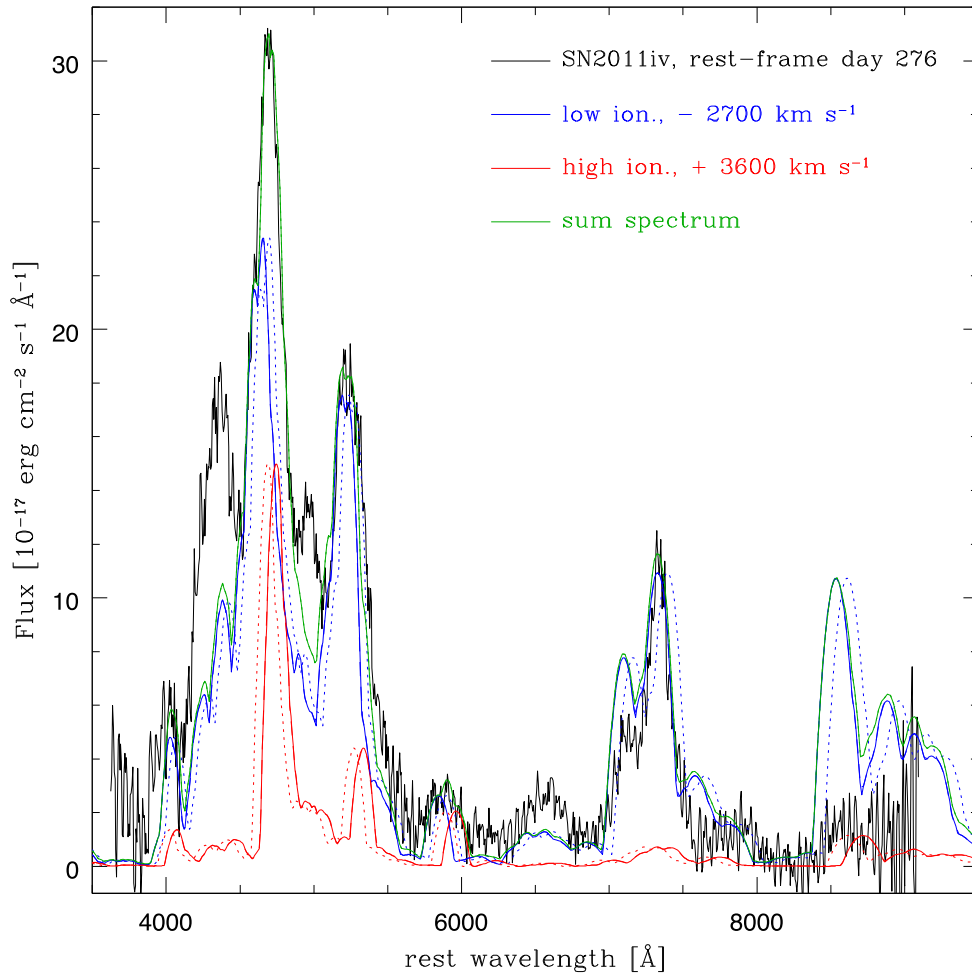
Figure 8. The nebular spectrum of SN 2011iv and the two-component model. The dotted lines show the two components at rest.

solution it has $v = 5000\,\mathrm{km\,s^{-1}}$, $M \sim 0.06\,\mathrm{M_\odot}$, and a redshift of $3600\,\mathrm{km\,s^{-1}}$, so that the line-of-sight velocity separation of the two components is $6300\,\mathrm{km\,s^{-1}}$, larger than in SN 2007on but compatible with the observed line width. The nebula is composed almost entirely of $^{56}\mathrm{Ni}$ ($0.06\,\mathrm{M_\odot}$), and it contains no stable Fe-group elements. Only traces of IMEs are present, essentially Na and Ca ($\sim 10^{-5}$–$10^{-4}\,\mathrm{M_\odot}$), which are necessary to give rise, in particular, to the red component of the Na I D/[Co III] feature (which is dominated by Na I D). The mass of this nebula is very small even when compared to the individual components in the spectrum of SN 2007on. It is actually comparable to the values of the emitting nebulae in SNe like 1991bg or 2003hv. Because of the much lower mass and density, this component has a much higher ionization degree than the blueshifted component, as shown by the ratio of the [Fe III]- and [Fe II]-dominated emissions.

The combined two-component model obtained by summing the blue- and redshifted components described above is shown in Fig. 8. Although it is not very different from the single-component models, whether one-zone or stratified (Ashall et al. 2018), it does match the observed line width better and it reproduces the shift of some lines.

The combination of the two components yields a $^{56}\mathrm{Ni}$ mass of $0.32\,\mathrm{M_\odot}$, which powers the light curve. This is not too different from what was derived from the peak of the light curve ($0.42\,\mathrm{M_\odot}$) by Gall et al. (2018) using a semi-analytic method. The total mass

included in the two nebulae (which have slightly different boundary velocities, 5000 and $5750\,\mathrm{km\,s^{-1}}$) is $0.52\,\mathrm{M_\odot}$. This is high for a standard-energy explosion, and comparable to the low-energy SN 1986G (Ashall et al. 2016a). This value is in line with the results of abundance tomography (Ashall et al. 2018), which also indicate that SN 2011iv had a low explosion energy and consequently a large mass at low velocity. The line-of-sight separation velocity, $6300\,\mathrm{km\,s^{-1}}$, is comparable to the expansion velocity of the two individual nebulae, which remain therefore at least partially spatially separated, and could be fully separated if the viewing angle was significantly different from the actual direction of motion. Of course both components are embedded in the much faster outer ejecta, which at early times may cause some light-curve broadening because of diffusion. Detailed modelling in three dimensions would be useful to test this.

Unlike the case of SN 2007on, in SN 2011iv the two components have very different masses, which makes the collisional scenario much less likely. The off-centre ignition scenario, on the other hand, could be viable. The blueshifted, 'low-ionization' component, which contains a significant fraction of stable Fe-group material, may correspond to the neutron-rich nucleosynthesis region that is predicted to occur in Chandrasekhar-mass models (Iwamoto et al. 1999), and which may be identified with the ashes of the centre of the WD. The redshifted, 'high-ionization' component does not contain neutron-rich species, and may correspond to the off-centre

component of the explosion. Regions of the WD that are sufficiently far removed from the centre are unlikely to be dense enough to synthesize neutron-rich species. In SN 2011iv the explosion may have started significantly off-centre, leading only to the synthesis of ^{56}Ni. The burning flame then propagated inwards causing the main explosion, which converted the innermost regions of the WD to neutron-rich species. The total mass seen within the boundary expansion velocities surveyed by the nebular spectra is high for a normal-energy Chandrasekhar-mass model, but could be in line with a low-energy explosion, which is shown to produce the best fits to the early-time spectra and the light curve in a companion paper (Ashall et al. 2018). A high relative abundance of neutron-rich NSE species is expected if the explosion proceeded slowly, and is a common feature of both SN 2011iv and SN 1986G. The high bulk velocity of the two components would also indicate a rather non-central ignition point. The less massive off-centre component has the higher velocity, although the values we derived are quite far from balancing momentum.

Finally, as this is possibly the first time SN Ia nebular spectra have been analysed with an approach that does not assume spherical symmetry of the ejecta, it is interesting to compare the properties of the spectra of SNe 2007on and 2011iv, in particular the shift of some of their emission lines, with their early-time spectral properties. Maeda et al. (2010) suggested that there is a link between the shift of the observed line that is identified as [Ni II] $\lambda 7378$ (and of another line identified as [Fe II] $\lambda 7155$) and the behaviour of the photospheric velocity at early times as described by the evolution of the velocity of Si II $\lambda 6335$, which is the defining line for SNe Ia. The sense of the relation is that the [Ni II] line is created in high neutron density ejecta where no ^{56}Ni is made and that corresponds to the region of the progenitor where burning occurred at the highest densities. This may be the centre, but may be slightly off-centre depending on where ignition first occurs. If burning starts off-centre the region that is initially affected will start to expand and move with some characteristic velocity, which will be reflected along the line of sight by an observed shift of the [Ni II] emission line. Maeda et al. (2010) found that when this line is blueshifted the early velocity evolution is slow [a 'low velocity gradient' (LVG) SN in the definition of Benetti et al. 2005]. Conversely, when the line is redshifted the early velocity evolution is fast [a 'high velocity gradient' (HVG) SN in the definition of Benetti et al. 2005]. This may suggest that the explosion stretches out the progenitor more in the direction opposite that of the region where burning begins. If SNe Ia do behave generically this way off-centre delayed detonations may be a common scenario.

For SN 2007on, Maeda et al. (2010) report a Si II velocity gradient of ≈ 85 km s^{-1} d^{-1}, which makes it almost a HVG SN, and no shift in the emission lines. The SN appears to be an outlier in their distribution. Given the scenario that we adopted for SN 2007on, namely the collision of two WDs, it would be natural to expect that some shift should be observed, as it is indeed for many other lines. We have found, however, that the [Ni II] line is very weak in SN 2007on, and the emission near 7380 Å is a blend of red- and blueshifted [Ca II], so we do not expect the relation to hold, which is indeed the case. The velocity gradient at early times is caused by the side of the ejecta that face us. If we look at the blueshifted nebula in our model, this has a velocity of 4200 km s^{-1}, which is extreme when looking at fig. 2 of Maeda et al. (2010). Therefore, even if we only consider the blueshifted component of the nebular spectrum, SN 2007on does not fit in the relation of Maeda et al. (2010). This may be seen as evidence supporting a different explosion scenario for SN 2007on.

As for SN 2011iv, we suggest here that this is likely to be an off-centre delayed detonation. It should therefore be the ideal candidate to test the scenario of Maeda et al. (2010). Ashall et al. (2018) find for SN 2011iv a Si II velocity gradient of 120 ± 20 km s^{-1} d^{-1}, which places it squarely among the HVG events. These are thought to be show redshifted [Ni II] emission lines. The [Ni II] line in SN 2011iv, however, is actually blueshifted by ~ 2700 km s^{-1}. Again, this SN does not seem to follow the relation suggested by Maeda et al. (2010). While this does not mean that SN 2011iv could not be an off-centre delayed detonation, it may indicate that the relation of Maeda et al. (2010) is not always predictive. What may actually be off-centre is not the ignition point but rather the point of transition from a deflagration to a detonation (Fesen et al. 2007).

In conclusion, SN 2007on appears to be consistent with the explosion following the collision of two WDs. An alternative – but in our opinion less likely – scenario is a very off-centre delayed detonation of a Chandrasekhar-mass WD. This latter scenario is more likely to apply to SN 2011iv. It is quite likely that most, if not all, physically motivated mechanisms that have been proposed do actually exist. Both direct collisions and off-centre delayed detonations may be more common among fast decliners. Our task is then to identify possible observed counterparts for these mechanisms. Being able to distinguish between different progenitor/explosion channels would greatly help with regards to using SNe Ia as cosmological standardizable candles. Nebular spectroscopy is a very useful tool to investigate the inner workings of SNe Ia.

REFERENCES

Ashall C., Mazzali P., Sasdelli M., Prentice S. J., 2016a, MNRAS, 460, 3529
Ashall C., Mazzali P. A., Pian E., James P. A., 2016b, MNRAS, 463, 1891
Ashall C. et al., 2018, MNRAS, preprint (arXiv:1802.09460)
Benetti S. et al., 2005, ApJ, 623, 1011
Burns C. R. et al., 2014, ApJ, 789, 32
Conley A. et al., 2006, AJ, 132, 1707
Cristiani S. et al., 1992, A&A, 259, 63
Dan M., Guillochon J., Brüggen M., Ramirez-Ruiz E., Rosswog S., 2015, MNRAS, 454, 4411
Dong S., Katz B., Kushnir D., Prieto J. L., 2015, MNRAS, 454, L61
Fang X., Thompson T. A., Hirata C. M., 2017, MNRAS, preprint (arXiv:1709.08682)
Fesen R. A., Höflich P. A., Hamilton A. J. S., Hammell M. C., Gerardy C. L., Khokhlov A. M., Wheeler J. C., 2007, ApJ, 658, 396
Filippenko A. V. et al., 1992a, ApJ, 384, L15
Filippenko A. V. et al., 1992b, AJ, 104, 1543
Foley R. J. et al., 2012, ApJ, 753, L5

Franx M., Illingworth G., Heckman T., 1989, ApJ, 344, 613
Gall C. et al., 2018, A&A, preprint (arXiv:1707.03823)
Gamezo V. N., Khokhlov A. M., Oran E. S., 2005, ApJ, 623, 337
Ganeshalingam M., Li W., Filippenko A. V., 2011, MNRAS, 416, 2607
Hamuy M., Trager S. C., Pinto P. A., Phillips M. M., Schommer R. A., Ivanov V., Suntzeff N. B., 2000, AJ, 120, 1479
Hayden B. T. et al., 2010, ApJ, 712, 350
Höflich P., Gerardy C. L., Fesen R. A., Sakai S., 2002, ApJ, 568, 791
Howell D. A., 2001, ApJ, 554, L193
Hsiao E. Y. et al., 2015, A&A, 578, A9
Iben I. J., Tutukov A. V., 1984, ApJS, 54, 335
Iwamoto K., Brachwitz F., Nomoto K., Kishimoto N., Umeda H., Hix W. R., Thielemann F.-K., 1999, ApJS, 125, 439
Kushnir D., Katz B., Dong S., Livne E., Fernández R., 2013, ApJ, 778, L37
Leibundgut B. et al., 1993, AJ, 105, 301
Leloudas G. et al., 2009, A&A, 505, 265
Livne E., 1990, ApJ, 354, L53
Livne E., Arnett D., 1995, ApJ, 452, 62
Livne E., Glasner A. S., 1991, ApJ, 370, 272
Maeda K. et al., 2010, Nature, 466, 82
Mazzali P. A., Hachinger S., 2012, MNRAS, 424, 2926
Mazzali P. A., Danziger I. J., Turatto M., 1995, A&A, 297, 509
Mazzali P. A., Chugai N., Turatto M., Lucy L. B., Danziger I. J., Cappellaro E., della Valle M., Benetti S., 1997, MNRAS, 284, 151
Mazzali P. A., Cappellaro E., Danziger I. J., Turatto M., Benetti S., 1998, ApJ, 499, L49
Mazzali P. A., Röpke F. K., Benetti S., Hillebrandt W., 2007, Science, 315, 825
Mazzali P. A., Sauer D. N, Pastorello A., Benetti S., Hillebrandt W., 2008, MNRAS, 386, 1897
Mazzali P. A., Maurer I., Valenti S., Kotak R., Hunter D., 2010, MNRAS, 408, 87
Mazzali P. A., Maurer I., Stritzinger M., Taubenberger S., Benetti S., Hachinger S., 2011, MNRAS, 416, 881
Mazzali P. A. et al., 2015, MNRAS, 450, 2631
Milne P. A. et al., 2010, ApJ, 721, 1627
Motohara K. et al., 2006, ApJ, 652, L101
Nomoto K., 1982, ApJ, 253, 798
Nomoto K., Kondo Y., 1991, ApJ, 367, L19
Pakmor R., Kromer M., Röpke F. K., Sim S. A., Ruiter A. J., Hillebrandt W., 2010, Nature, 463, 61
Pakmor R., Hachinger S., Röpke F. K., Hillebrandt W., 2011, A&A, 528, A117
Pastorello A. et al., 2007, MNRAS, 377, 1531
Phillips M. M., 1993, ApJ, 413, L105
Phillips M. M. et al., 1987, PASP, 99, 592
Phillips M. M., Wells L. A., Suntzeff N. B., Hamuy M., Leibundgut B., Kirshner R. P., Foltz C. B., 1992, AJ, 103, 1632
Phillips M. M., Lira P., Suntzeff N. B., Schommer R. A., Hamuy M., Maza J., 1999, AJ, 118, 1766
Raskin C., Scannapieco E., Rockefeller G., Fryer C., Diehl S., Timmes F. X., 2010, ApJ, 724, 111
Roelofs G., Bassa C., Voss R., Nelemans G., 2008, MNRAS, 391, 290
Rosswog S., Kasen D., Guillochon J., Ramirez-Ruiz E., 2009, ApJ, 705, L128
Sasdelli M., Mazzali P. A., Pian E., Nomoto K., Hachinger S., Cappellaro E., Benetti S., 2014, MNRAS, 445, 711
Scott N., Davies R. L., Houghton R. C. W., Cappellari M., Graham A. W., Pimbblet K. A., 2014, MNRAS, 441, 274
Sullivan M. et al., 2010, MNRAS, 406, 782
Voss R., Nelemans G., 2008, Nature, 451, 802
Webbink R. F., 1984, ApJ, 277, 355
Whelan J., Iben I. J., 1973, ApJ, 186, 1007
Woosley S. E., Weaver T. A., 1994, ApJ, 423, 371
Zhang J.-J. et al., 2016, ApJ, 817, 114

This paper has been typeset from a TeX/LaTeX file prepared by the author.